

## Positional screening and NMR structure determination of side-chain-to-side-chain cyclized $\beta^3$ -peptides†

Esther Vaz,<sup>a</sup> Sonja A. Dames,<sup>b</sup> Matthias Geyer<sup>\*a</sup> and Luc Brunsveld<sup>\*a,c</sup>

Received 19th August 2011, Accepted 7th November 2011

DOI: 10.1039/c1ob06422c

Many  $\beta$ -peptides fold in a 14-helical secondary structure in organic solvents, but similar 14-helix formation in water requires additional stabilizing elements. Especially the 14-helix stabilization of short  $\beta$ -peptides in aqueous solution is critical, due to the limited freedom for incorporating stabilizing elements. Here we show how a single lactam bridge, connecting two  $\beta$ -amino acid side-chains, can lead to high 14-helix character in short  $\beta^3$ -peptides in water. A comparative study, using CD and NMR spectroscopy and structure calculations, revealed the strong 14-helix inducing power of a side-chain-to-side-chain cyclization and its optimal position on the  $\beta^3$ -peptide scaffold with respect to pH and ionic strength effects. The lactam bridge is ideally incorporated in the N-terminal region of the  $\beta^3$ -peptide, where it limits the conformational flexibility of the peptide backbone. The lactam bridge induces a 14-helical conformation in methanol and water to a similar extent. Based on the presented first high resolution NMR 3D structure of a lactam bridged  $\beta^3$ -peptide, the fold shows a large degree of high order, both in the backbone and in the side-chains, leading to a highly compact and stable folded structure.

### Introduction

The design and synthesis of oligomeric structures that can fold and adopt predictable and stable conformations in solution, called foldamers, has received significant attention.<sup>1</sup> The controlled folding of synthetic molecules in aqueous solutions is an especially important goal, since such predictable and stable secondary structures are attractive for the generation of biologically active molecules.<sup>2</sup>  $\beta$ -Peptides, which are composed of homologated  $\beta$ -amino acids, provide a good scaffold for the design of foldamers, since a wide-variety of monomeric building blocks is accessible and the resulting oligomers can form a plethora of secondary structures.<sup>3</sup> One of the most studied  $\beta$ -peptide secondary structures is the 14-helix.<sup>4</sup> This oligoamide helix is defined by the formation of  $i, i-2$  C=O...H-N backbone hydrogen bonds, in a 14-atom ring. As a result every third residue has the same position along the outside of the helix. The folding of  $\beta$ -peptides into 14-helices has attracted significant attention, both from a

structural point of view and as well-defined scaffolds for the design of protein interaction modules<sup>5</sup> and possible antibacterial or antifungal agents.<sup>6</sup>

For a number of biological applications, the stabilization of short  $\beta$ -peptides with stable helical folds in aqueous buffers is of particular interest. Several design strategies have been developed to address the stabilization of 14-helix folding in water. The vast majority of these strategies make use of the fact that the amino acid side-chains in the  $i$  and  $i+3$  positions are located in close proximity on the outside of the helix and therefore can be utilized for physical or chemical stabilization of the 14-helical fold. The first reports of 14-helix stabilization in water were shown with  $\beta$ -peptides incorporating six-membered ring constrained residues, such as *trans*-2-aminocyclohexanecarboxylic acid.<sup>7</sup> These residues feature a preferred conformation, highly beneficial for 14-helix formation. A number of groups have shown that 14-helix formation in  $\beta$ -peptides exclusively built up of  $\beta^3$ -amino acids could be achieved by oppositely charged side-chains at the  $i$  and  $i+3$  positions.<sup>8</sup> It has further been reported that additional stabilization of the helical fold can be achieved by favourable interactions of the charged side-chains with the helix macrodipole, *i.e.* basic residues near the N-terminus and acidic residues near the C-terminus. Subsequent studies have shown that residues with side-chain branching adjacent to the backbone, such as  $\beta^3$ -homovaline ( $\beta^3$ -hVal) promote 14-helicity and can replace some of the charged side-chains, reducing the number of required electrostatic side-chain interactions from two to only one face of the helix.<sup>9</sup> In analogy with  $\alpha$ -helix stabilization strategies for

<sup>a</sup>Max Planck Institute of Molecular Physiology, Otto-Hahn Strasse 11, 44227, Dortmund, Germany. E-mail: matthias.geyer@mpi-dortmund.mpg.de

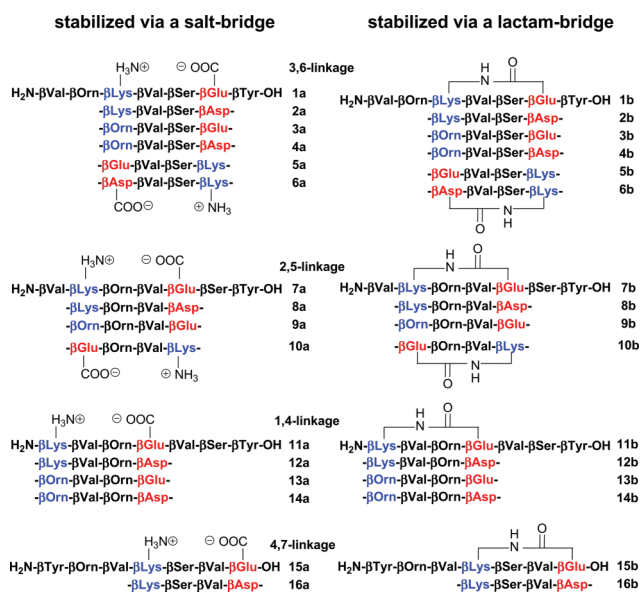
<sup>b</sup>TU München, Lichtenbergstrasse 4, 85747, Garching, Germany

<sup>c</sup>Laboratory of Chemical Biology, Department of Biomedical Engineering, TU Eindhoven, Den Dolech 2, 5612AZ, Eindhoven, The Netherlands. E-mail: l.brunsveld@tue.nl; Fax: (+31)40-2478367

† Electronic supplementary information (ESI) available: experimental details, additional CD data and 1D/2D NMR spectra. See DOI: 10.1039/c1ob06422c

$\alpha$ -peptides,<sup>10</sup> covalent linking of side-chains at the *i* and *i*+3 positions in  $\beta^3$ -peptides was also shown to be highly effective for 14-helix stabilization. Disulfide bridging of two side-chains represented the first example in this respect, leading to 14-helix stabilization in methanol.<sup>11</sup> Strong stabilization of 14-helical structures in water was first achieved by covalent linkage of side-chain residues by amide bonds.<sup>12</sup> More recently, stable 14-helices in aqueous solution were prepared using ring-closing metathesis to connect the side-chains of non-natural homologated amino acids.<sup>13,14</sup> Based on this work, the first NMR solution-structure analysis of a constrained peptide was presented.<sup>13</sup>

Each type of 14-helix stabilization strategy has its specific advantages, for example with respect to synthetic access or helix stability.<sup>12b</sup> 14-Helix stabilization of  $\beta^3$ -peptides by covalent side-chain linkages appears to require only one bridge element for the induction of helicity in a peptide of average length.<sup>12</sup> Covalent linkage of the side-chains lowers the pH and salt concentration sensitivity of the helical fold. The more hydrophobic nature of the 14-helix, introduced by virtue of the covalent bridge, might further favor cellular uptake.<sup>14b</sup> As a result, covalent side-chain bridging appears to be a favorable approach, especially for the stabilization of short 14-helix motifs in  $\beta^3$ -peptides. Concomitantly, molecular details on the exact placement and structural characteristics of the side-chain stabilized short 14-helices are required to guide the design of biologically active analogues. Here we describe the design of a set of heptameric, linear and cyclized peptides composed of  $\beta^3$ -amino acids and their structural characteristics concerning 14-helix stability. Special focus is on the placement of the side-chain-to-side-chain lactam bridge within the  $\beta^3$ -peptide scaffold. The generated library of salt and lactam bridged  $\beta^3$ -peptides (Scheme 1) was structurally characterized by CD and NMR spectroscopy. This approach resulted in an optimized stable 14-helical platform for short  $\beta^3$ -peptides.



**Scheme 1** Library of heptameric  $\beta^3$ -peptides (**1–16**) containing either electrostatic side-chain interactions (**a** series) or a covalent amide bridge (**b** series) positioned at different linkage locations in the  $\beta^3$ -peptide from the N- to the C-terminus.

## Design and synthesis

A small family of 20 heptameric  $\beta^3$ -peptides (Scheme 1, **1–10**) has been previously designed to study if rigidification of the backbone structure by electrostatic interactions or by side-chain-to-side-chain lactam bridges promotes folding into 14-helical conformations.<sup>12</sup> In order to assess the helix stabilizing efficacy of both strategies, the rigidification elements were varied in length, position, and orientation in the middle of the  $\beta^3$ -peptide sequences. Circular dichroism (CD) and NMR spectroscopy measurements showed that an appropriate covalent side-chain-to-side-chain linkage provided better helical structure stabilization in water than the corresponding salt-bridge interaction between side-chains. We observed that the seven to eight atom-bridge length (between  $\beta^3$ -Lys and  $\beta^3$ -Glu or  $\beta^3$ -Asp) and positioning of the covalent bridge nearer to the N-terminus of the  $\beta^3$ -peptide greatly favored folding into a 14-helix (**7b** and **8b**).<sup>12</sup> These results led us to undertake and report here a more detailed analysis of the optimal positioning of the amide side-chain linkage with respect to 14-helix inducing power. We therefore designed and prepared an enlarged library of heptameric, amide side-chain cyclized  $\beta^3$ -peptides (Scheme 1, **1–16**) with *i* to *i*+3 linkages at each of the possible positions within the  $\beta^3$ -peptides (1,4; 2,5; 3,6; 4,7). For comparison, the analogous salt-bridge stabilized  $\beta^3$ -peptides were also prepared. The conformations of the resulting peptides were analyzed by CD and NMR spectroscopy. Also we report here the first high resolution NMR 3D structure of a lactam bridged  $\beta^3$ -peptide.

The  $\beta^3$ -peptide library (Scheme 1) was prepared by solid-phase peptide synthesis on TentaGel R PHB resin, which has high swelling capacity and low initial loading, suitable for on-bead cyclizations. Allyloxycarbonyl carbamate (Alloc) and allyl ester were chosen as orthogonal protecting groups for the amine and carboxylic acid functional groups of the  $\beta^3$ -amino acids, respectively, which subsequently would form either the salt- or the covalent amide bridge.<sup>12</sup>  $\beta^3$ -Peptides **11–16** were newly synthesized using microwave irradiation and HBTU, HOBt and DIEA as coupling reagents. Piperidine in DMF was used for Fmoc cleavage. After complete assembly of the heptamer, the allyl and Alloc side-chain protecting groups were selectively removed with [Pd(Ph<sub>3</sub>)<sub>4</sub>] in dichloromethane and phenylsilane. For some of the  $\beta^3$ -peptides this led to a concomitant partial loss of the terminal Fmoc group, as detected *via* LC-MS. In these cases, in order to avoid isomer formation during the subsequent cyclization step, a Boc-protected  $\beta^3$ -amino acid was alternatively used as N-terminal building block, thus avoiding undesired liberation of the peptide N-terminus. The non-commercial Boc-protected  $\beta^3$ -amino acids were prepared *via* the Arndt–Eistert homologation method (see Supporting Information†).

After assembly and deprotection of the heptameric sequences, the  $\beta^3$ -peptide resin was divided into two batches for either salt-bridged stabilized  $\beta^3$ -peptide (*via* direct cleavage from the resin) or covalently rigidified  $\beta^3$ -peptide (*via* on-bead cyclization and subsequent cleavage from resin) formation. The on-bead cyclization for  $\beta^3$ -peptides **1b–10b** was previously reported by us to proceed smoothly using HATU and HOBt as cyclization reagents in NMP.<sup>12</sup> This method was also effective for the cyclization of peptides **15b** and **16b**. However, those conditions were found to be less effective for cyclization of peptides **11b–14b**, bearing the lactam bridge as a 1,4-linkage at the complete peptide N-terminus.

The cyclization in this case might be hindered due to a higher degree of conformational freedom at the complete end of the peptide sequence. Other coupling reagents such as PyBOP and BTFFH or the use of collidine as base instead of DIEA were all tested, but did not improve the cyclization efficiency. In order to influence the conformation of the  $\beta$ -peptide during cyclization, several solvents were screened (NMP, DMF, 1 : 1 THF/NMP, 1 : 1 DCM/NMP, CH<sub>3</sub>CN). The usage of HATU with DIEA in 1 : 1 THF/NMP finally proved to be the best condition for on-bead cyclization at the N-terminus of the peptide sequence. Standard cleavage from resin using 96% TFA, water and TIPS required 3 h to reach a complete removal of the *t*Bu and Boc protecting groups. After preparative RP-HPLC purification the linear (30% average yield) and cyclic peptides (10% average yield) were obtained in moderate to good yields and high purity, as determined by LC-MS (see Supporting Information†).

### Structure analysis by CD spectroscopy

Circular dichroism (CD) measurements were performed on all  $\beta^3$ -peptides (1–16, **a** and **b** series) in both methanol and buffered water. The 14-helix of  $\beta^3$ -peptides typically shows a very characteristic CD signature composed of a maximum in the ellipticity around 195–198 nm and a minimum at 213–215 nm. From this conserved shape the 14-helical content of  $\beta^3$ -peptides with analogous sequences can be evaluated according to the mean residue ellipticity (MRE) at 215 nm.<sup>2,3</sup> Fig. 1 shows representative CD signatures of cyclic  $\beta^3$ -peptides from our library (~150  $\mu$ M) in methanol and in aqueous 10 mM sodium-phosphate buffer, pH 7.4. In methanol

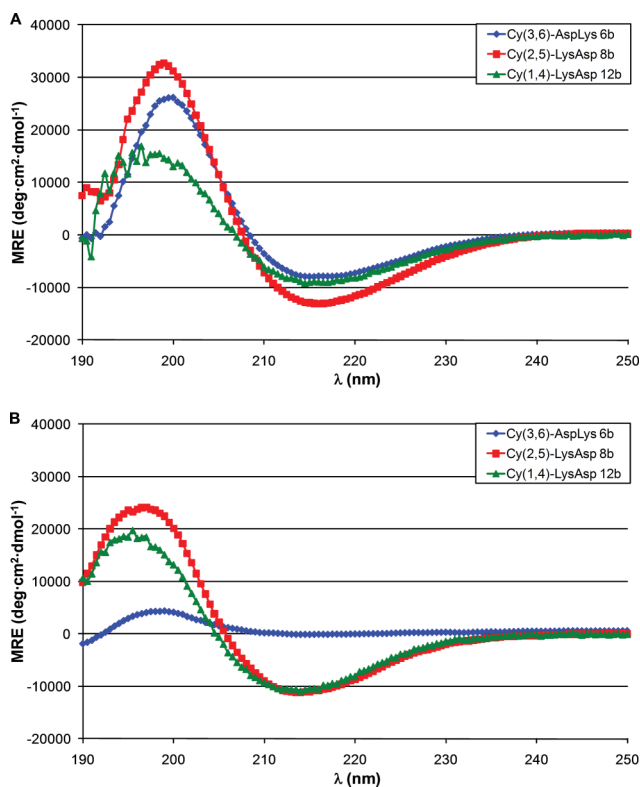


**Fig. 1** CD signatures of cyclic  $\beta^3$ -peptides **6b**, **8b**<sup>12</sup> and **12b** (~150  $\mu$ M) in methanol (A) and in aqueous 10 mM sodium-phosphate buffer at pH 7.4 (B). All measurements were performed at 20 °C.

(Fig. 1A), all linear and cyclic peptides showed CD signatures characteristic for 14-helix formation with MRE values at 215 nm of about  $-10\,000$  deg cm<sup>2</sup> mol<sup>-1</sup> (see also Supporting Information†). This suggests that all  $\beta^3$ -peptides display significant and similar extents of 14-helicity in this helix-stabilizing solvent. For most of the  $\beta^3$ -peptides in methanol, the 14-helix inducing power of the lactam bridge is slightly lower compared to that of the salt-bridge. In organic solvent, both the bridge type and position thus have only minor effects on the 14-helicity in the respective  $\beta^3$ -peptides.

In aqueous solution (pH 7.4) more significant and striking differences were observed between the linear and cyclic peptides as well as within the specific sub-libraries. In water the position and type of bridge element significantly influenced the 14-helical character of the  $\beta^3$ -peptides (Fig. 1B, Fig. 2).

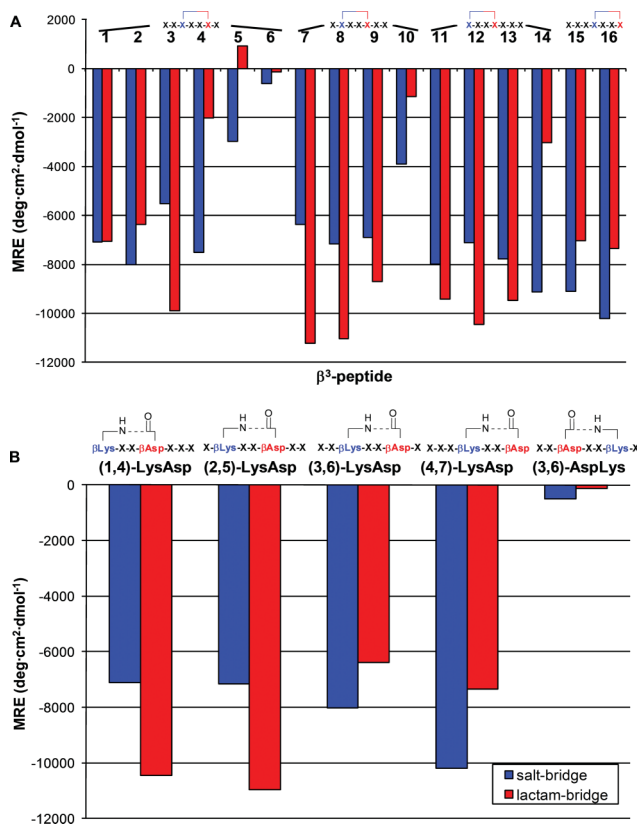


**Fig. 2** (A) Effect of the type (blue = salt-bridge; red = lactam-bridge) and position of the bridge on the helical structure observed by CD measurements at 215 nm in water (aqueous 10 mM sodium-phosphate buffer at pH 7.4); and (B) visualization of the specific N-terminal preference for the lactam bridge in the cyclic peptides and C-terminal preference of the salt bridge element in linear peptides. All measurements were performed at 20 °C and ~150  $\mu$ M  $\beta^3$ -peptide concentration.

First, the orientation of the bridge has a radical effect on 14-helix stability.  $\beta^3$ -Peptides **5**, **6**, and **10** showed a complete absence of 14-helical structure. In these  $\beta^3$ -peptides, the  $\beta^3$ -hLys of the bridge motif is positioned towards the C-terminus and the  $\beta^3$ -hAsp, or  $\beta^3$ -hGlu component towards the N-terminus. For example, for Lin(3,6)-AspLys (**6a**) and Cy(3,6)-AspLys (**6b**), respectively, the MRE values fall to  $-500$  and  $-100$  deg cm<sup>2</sup> dmol<sup>-1</sup>. Thus, the orientation of the bridging partners along the sequence has a large impact on the stability of both, the salt- and the



lactam-bridged peptides. The interactions of side-chains with the helical macrodipole play an important role in the stabilization of 14-helices.<sup>9</sup> The H-bonding pattern within the 14-helix generates a macrodipole with a partial positive charge at the C-terminus and concomitant negative charge at the N-terminus. For the salt-bridge stabilized  $\beta^3$ -peptides, the localization of a positively charged residue close to the C-terminus, as in  $\beta^3$ -peptides **5a**, **6a**, and **10a**, thus interferes with the 14-helix macrodipole. Similarly and in line with results observed for  $\alpha$ -peptides,<sup>15</sup> the direction of the dipole of the lactam bridge is also influencing 14-helix stability. For  $\beta^3$ -peptides **5b**, **6b**, and **10b** an unfavorable dipole interaction is expected, which analogously to their linear counterparts, acts destabilizing on the 14-helix structure.

Second, the length of the side-chains in the bridging elements has a significant influence on 14-helix formation in the cyclic lactam bridged  $\beta^3$ -peptides. Indicated by the very low MRE values for  $\beta^3$ -peptides **4** and **14**, the shortest lactam bridge element between a  $\beta^3$ -hOrn and a  $\beta^3$ -hAsp turned out to be detrimental for 14-helix formation. Apparently, a short lactam bridge does not match the molecular requirements for H-bond formation in the 14-helix. Most probably, the short linker induces significant constraints in the folded peptide, counteracting the 14-helix folding motif. In contrast, those cyclic  $\beta^3$ -peptides with longer lactam bridges, featuring either at least a  $\beta^3$ -hLys or a  $\beta^3$ -hGlu, all showed high 14-helicity, in many cases surpassing the 14-helicity induced by the equivalent salt bridge. When the lactam bridge is provided with enough molecular flexibility, by virtue of longer side-chains, the bridging element nicely complements the 14-helix folding motif (*vide infra* NMR results) leading to large MRE values. Small variations in the MRE values between the different longer linker types probably resulted from effects such as differences in the polarity of the newly introduced amide bond and its interaction with the  $\beta^3$ -peptide surface. For the salt bridge stabilized  $\beta^3$ -peptides the side-chain lengths ( $\beta^3$ -hLys *vs.*  $\beta^3$ -hOrn and  $\beta^3$ -hGlu *vs.*  $\beta^3$ -hAsp) had overall only a minor effect on the stability of the 14-helix, reflecting a higher side-chain flexibility.

Third, the relative positioning of the bridging element along the  $\beta^3$ -peptide scaffold influences its 14-helix stability. The results shown in Fig. 2 demonstrate that a favorable proximity of the bridge to a specific  $\beta^3$ -peptide terminus exists, albeit with different preferences for the two bridge types. Cyclic  $\beta^3$ -peptides featuring an appropriate lactam bridge close to the N-terminus, *i.e.* between positions 1,4 (**11b–13b**) and 2,5 (**7b–9b**), typically exhibit strong MRE values at 215 nm, indicating significant 14-helix character. Compared to the cyclic lactam series at positions 3,6 and 4,7 ( $\beta^3$ -peptides **1b–6b** and **15b–16b**) and compared to their open chain salt bridge analogues (**7a–9a** and **11a–13a**),  $\beta^3$ -Peptides **7b–9b** and **11b–13b** showed the highest 14-helical content in water with MRE values at 215 nm in the range of  $-10\,000\text{ deg cm}^2\text{ dmol}^{-1}$ . Indeed,  $\beta^3$ -peptides **7b** and **8b** even feature MREs of  $-11\,000\text{ deg cm}^2\text{ dmol}^{-1}$ , constituting the highest 14-helical content of all  $\beta^3$ -peptides in water characterized in this study. Furthermore the MRE values of the lactam-bridged  $\beta^3$ -peptides in water have not diminished with respect to the MRE value in methanol. This illustrates the high stability of the lactam-bridged 14-helix structures upon going from a helix stabilizing solvent, such as methanol, to water.

In contrast to the lactam-bridged  $\beta^3$ -peptides, the salt bridged versions showed an opposite behavior regarding the sequential positioning of the bridging element. In the (3,6) series ( $\beta^3$ -

peptides **1–3**) MRE values are comparable between the cyclic and linear variants, although the lactam bridge variant of **3** (**3b**) features a notably higher 14-helical character than its salt-bridge counterpart. However in the (4,7) series, the salt-bridge stabilized  $\beta^3$ -peptides outcompete the lactam-bridge stabilized  $\beta^3$ -peptides. These results demonstrate that ionic side-chain interactions result in increasing stabilities of the secondary structure when the bridge is located close to the C-terminus of the  $\beta^3$ -peptide. Clearly, these observations are supposed to result from a number of molecular interactions operating simultaneously within the  $\beta^3$ -peptide. For the salt-bridge series, positioning of the negatively charged  $\beta^3$ -hGlu or  $\beta^3$ -hAsp close to the  $\beta^3$ -peptide C-terminus is probably highly effective in stabilizing the macrodipole of the 14-helix. It has been reported that when positioned more centrally on the linear  $\beta^3$ -peptide, a basic side-chain is moderately stabilizing, whereas an acidic side-chain is slightly destabilizing.<sup>9c</sup> In line with this observation, the  $\beta^3$ -peptides with salt bridges between positions 1,4 and 2,5 (**11a–14a** and **7a–10a**) are less stable than the 4,7 analogues (**15a–16a**), which feature a  $\beta^3$ -hLys in the middle of the sequence and  $\beta^3$ -hGlu at its C-terminus. For the lactam bridged series, the intrinsic flexibility of the  $\beta^3$ -peptide is expected to be much more important for the helix stability than charge effects. In this respect it has been reported that in  $\beta^3$ -peptides, the N-terminus typically features a lower population of H-bonding than the C-terminus.<sup>9c</sup> Stabilizing effects imposed by side-chain cyclization are thus expected to be more pronounced when positioned near the N-terminus. This is especially eminent in short  $\beta^3$ -peptides, as studied here, since these will intrinsically be less structured than previously studied longer  $\beta^3$ -peptides.<sup>8,9</sup> Consistent with these observations, optimal helix stabilization of the short  $\beta^3$ -peptides analyzed here is achieved by using a covalent lactam bridge near the N-terminus.

## pH and salt stability

The effect of changes in the environmental conditions on 14-helicity for either type of bridging element was evaluated from CD spectroscopy measurements at different pH values and salt concentrations. For the selected  $\beta^3$ -peptides **7**, **9**, **12**, and **16**, pH dependent measurements were performed in the regime between pH 1.7 and 9.6 (Fig. 3). Analysis of the characteristic intensities at 215 nm showed appreciable pH sensitivity of both the linear and cyclic  $\beta^3$ -peptides. All  $\beta^3$ -peptides showed a significant decrease of

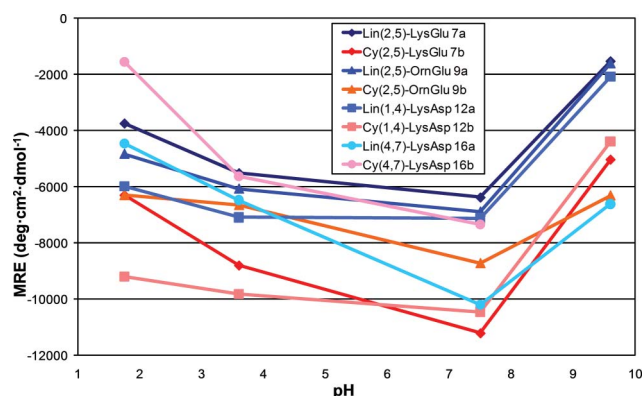


Fig. 3 MRE values at 215 nm of  $\beta^3$ -peptides **7**, **9**, **12**, and **16** for the pH-range from 1.7 to 9.6.

14-helicity when increasing the pH from 7.4 to 9.6. Lowering the pH to 3.6 or even 1.8 instead had a smaller effect on the 14-helix population. The destabilizing effect of high and low pH on 14-helix stability probably relates to changes in the protonation states of the amine and carboxylate functionalities within the  $\beta^3$ -peptides. Especially the destabilizing interaction of the different protonated states of the terminal amine and carboxylic groups with the 14-helix macrodipole, common to both the linear and cyclic  $\beta^3$ -peptides, is playing a major role for the effect. Nevertheless, almost all lactam-stabilized peptides were more stable than the corresponding salt-bridge stabilized peptides over the whole pH regime. The only exception in this respect is  $\beta^3$ -peptide **16b** for which the bridging element is positioned between residues 4 and 7.

The folding of the  $\beta^3$ -peptides of this study is stabilized in part by electrostatic interactions. The importance of electrostatic interactions on 14-helix stability can be screened by increasing the salt concentrations (e.g. NaCl). If the fold of a particular  $\beta^3$ -peptide is significantly stabilized by electrostatic interactions, it is expected to be destabilized in the presence of high salt concentrations.<sup>5,12</sup> Fig. 4 shows the influence of increasing the NaCl concentration from 0 to 1.6 M on the MRE at 215 nm for a selected set of salt- and lactam-bridged  $\beta^3$ -peptides that all have stabilizing element located near the N-terminus. For all studied  $\beta^3$ -peptides the MRE decreased with increasing concentration of the electrolyte. As expected, the salt effect is significantly more pronounced for the  $\beta^3$ -peptides with an intrahelical salt bridge as 14-helix stabilizing element. Accordingly,  $\beta^3$ -peptides **8a** and **12a**, showed a rapid decrease of the helical content upon increasing the electrolyte concentration. In the presence of 1.6 M sodium chloride the negative MRE values at 215 nm have diminished by 70%, indicating that reduction of the ionic interaction by high salt greatly destabilizes the 14-helical fold.  $\beta^3$ -Peptides **8b** and **12b**, bearing a side-chain-to-side-chain covalent bond, showed only a decrease of 39% at the highest electrolyte concentration, suggesting that the 14-helical structure is still significantly populated. The observed destabilization of the lactam-bridged  $\beta^3$ -peptides at high salt results probably from a charge-macrodipole interaction (see above, pH screening).

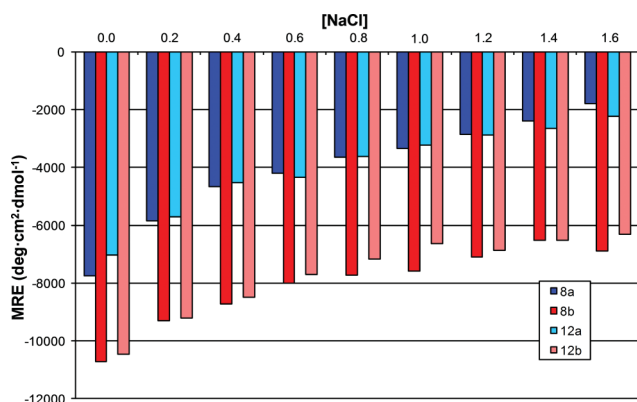


Fig. 4 MRE values at 215 nm for  $\beta^3$ -peptides **8** and **12** in aqueous buffer at NaCl concentrations from 0 to 1.6 M.

### Structure analysis by NMR spectroscopy

The high 14-helix stability of some of the lactam-bridged  $\beta^3$ -peptides argued for a more detailed structural analysis of selected

$\beta^3$ -peptides by NMR spectroscopy. Initially, two sets of  $\beta^3$ -peptides, **6a,b** and **8a,b**, were selected because of their opposite structural characteristics in aqueous solution as indicated by the CD data. Based on the MRE values at 215 nm,  $\beta^3$ -peptides **6a,b** showed a complete absence of 14-helix structure, whereas  $\beta^3$ -peptides **8a,b**, especially **8b**, showed a high degree of 14-helicity. An initial indication whether the  $\beta^3$ -heptapeptides under study form an ordered secondary structure can be obtained from the degree of the dispersion of NMR signals. <sup>1</sup>H-NMR experiments of  $\beta^3$ -peptides **6a**, **6b**, **8a** and **8b** were obtained in buffered water solution at 10 °C (Fig. 5). The cyclic peptides **6b** and **8b** showed overall a greater dispersion of amide proton signals than their linear counterparts **6a** and **8a**, respectively. For  $\beta^3$ -peptides **6a** and **6b**, some of the amide proton signals (i.e. at 8.10 and 8.19 ppm) are exchange broadened. This observation could be explained by conformational averaging between different secondary structures or between a folded and unfolded state. These results provide another hint toward the instability of potential 14-helical structure and are in line with the absence of 14-helix signature in the CD spectra of the respective  $\beta^3$ -peptides in water. In contrast, for  $\beta^3$ -peptides **8a** and **8b**, all amide protons, including the amide proton of the lactam bridge in **8b**, can be detected as about equally intense signals. This indicates a much more stable fold for these  $\beta^3$ -peptides and most likely a 14-helix in agreement with the observed CD data. Consistent with the larger absolute value of the MRE at 215 nm for the cyclic  $\beta^3$ -peptide **8b**, which indicates higher 14-helix stability, it also shows a greater dispersion of the NMR signals compared to the linear peptide **8a**.

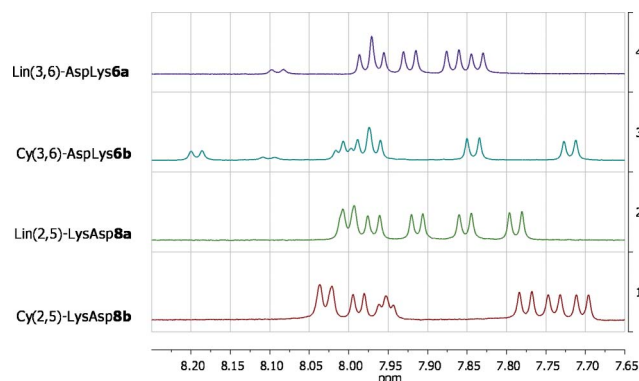
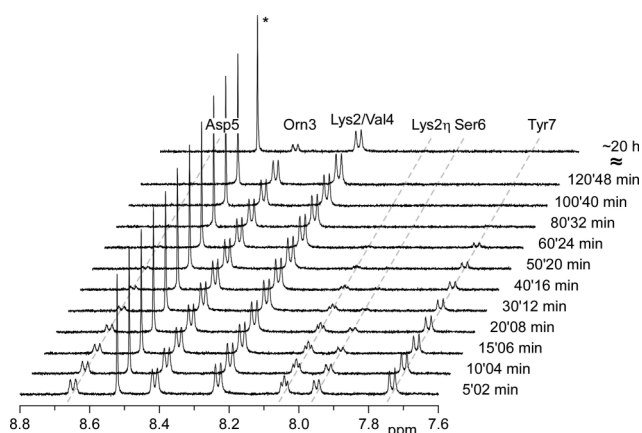


Fig. 5 NH region of  $\beta^3$ -peptides **6a**, **6b**, **8a** and **8b** in H<sub>2</sub>O/D<sub>2</sub>O 9:1 at pH 7.4 and 10 °C.

The H/D exchange rates of amide protons with solvent protons are sensitive to the secondary structure content of the peptide in solution. A low exchange rate indicates that protons are shielded from interaction with the bulk water by an ordered structure, e.g. by a hydrogen bonded helix. In contrast, a fast H/D exchange indicates the amide to be readily accessible to the solvent, either because of an unfolded nature or because of rapid interchange between different conformations. Because CD measurements for  $\beta^3$ -peptide **8b** indicated a high degree of 14-helix secondary structure in methanol and water, its H/D exchange rates were determined.<sup>16</sup> A time course series of <sup>1</sup>H-NMR spectra of  $\beta^3$ -peptide **8b** dissolved in CD<sub>3</sub>OD at 2 °C was obtained (Fig. 6). Initial rapid recordings of the <sup>1</sup>H-NMR spectra showed all seven amide proton signals of **8b** in the regime between 7.6 and 8.8 ppm.



**Fig. 6** H/D exchange series of  $\beta^3$ -peptides Cy(2,5)-LysAsp (**8b**) in 100%  $\text{CD}_3\text{OD}$  at 2 °C. The peak at 8.52 ppm (labeled \*) corresponds to formic acid.

In time, the amide protons exchange for deuterium, leading to a decrease in amide proton signal intensity. The observed H/D exchange half-times range from about 15 min to over 20 h. A clear difference in H/D exchange rates is observed for the different positions within the  $\beta^3$ -peptide. Whereas, the flanking amide bonds and also the lactam bridge exchange more rapidly, the residues embedded between the macrocyclic lactam system,  $\beta^3$ -hLys2,  $\beta^3$ -hOrn3, and  $\beta^3$ -hVal4, showed very long H/D exchange half-times indicative of a very stable conformation in this region.

To further assess the structure of the  $\beta^3$ -peptides in solution and to analyze their helical character, homonuclear 2D NMR spectra were recorded for a number of  $\beta^3$ -peptides (**8a**, **8b**, **12b**), both in methanol and in aqueous solvent. Total correlation spectroscopy (TOCSY) experiments were acquired to identify the characteristic residue spin systems of the  $\beta^3$  amino acids and to assign the proton resonances (Table 1 and Supporting Information†). The obtained assignments were confirmed based on intrasidues and sequential NOE-connectivities from ROESY experiments recorded with mixing times of 150 and 300 ms (Fig. 7 and Supporting Information†). The ROESY spectra showed further medium-range NOEs characteristic for 14-helix structure, e.g. between amide protons and protons at  $\beta$ -positions two or three residues apart ( $[\text{H}^{\text{N}}(i)-\text{H}^{\beta}(i+2)]$  and  $[\text{H}^{\text{N}}(i)-\text{H}^{\beta}(i+3)]$ ), or between  $\text{C}^{\alpha}$ -protons and  $\text{C}^{\beta}$ -protons three residues toward the C-

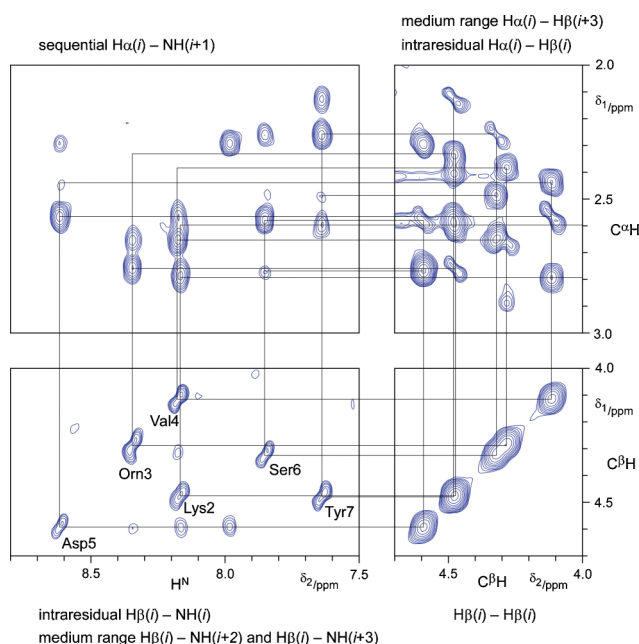


**Fig. 7** Sequential NOE path of the  $\beta^3$ -heptapeptide **8b** extracted from ROESY experiments in MeOH. Each quadrant highlights specific 14-helix characteristic, intrasidues and medium range correlations.

terminus,  $[\text{H}^{\alpha}(i)-\text{H}^{\beta}(i+3)]$ . Fig. 7 shows selected regions from the ROESY spectrum of  $\beta^3$ -peptide **8b** in methanol. In methanol as well as in water all proton signals could be observed and assigned. Furthermore, in both solvents the two protons attached to the  $\text{C}^{\alpha}$  carbons could be assigned stereo-specifically for the axial and equatorial position, supporting formation of secondary structure and a high degree of order in both solvents.

The conformational stability of  $\beta^3$ -heptapeptide **12b** in methanol was further assessed from temperature shift experiments. Going from 271 K to 283 K relative amide proton shift were as listed (in ppm): Lys1  $\text{H}^{\text{N}}$   $-0.07$ ; Val2  $-0.03$ ; Orn3  $-0.05$ ; Asp4  $-0.03$ ; Val5 0.00; Ser6  $-0.08$ ; Tyr7  $-0.09$  (see also Supporting Information†). The observation of negative temperature coefficients for the analyzed range of 12 K is in full agreement with those observed for the amide resonances of  $\alpha$ -peptides and proteins. Assuming a linear dependence of  $\text{H}^{\text{N}}$  shift versus temperature change, as has been observed previously,<sup>17</sup> the values of these

**Table 1**  $^1\text{H}$  NMR chemical shifts of the cyclic  $\beta^3$ -heptapeptide **8b** in aqueous solution or MeOH at 283 K

	Solvent	$\text{H}^{\text{N}}$	$\text{H}^{\alpha}_{\text{ax}}$	$\text{H}^{\alpha}_{\text{eq}}$	$\text{H}^{\beta}$	$\text{H}^{\gamma}$	Others
$\beta^3$ -Val1	$\text{H}_2\text{O}$	—	2.58	2.65	3.32	1.84	$\delta\text{CH}_3$ : 0.87
	MeOH	—	2.80	2.60	3.42	2.00	$\delta\text{CH}_3$ : 1.05
$\beta^3$ -Lys2	$\text{H}_2\text{O}$	8.02	2.50	2.29	4.09	1.49, 1.51	$\delta\text{CH}_2$ : 1.18, 1.22; $\varepsilon\text{CH}_2$ : 1.37 $\zeta\text{CH}_2$ : 3.02, 3.07; $\eta\text{NH}$ : 7.94
	MeOH	8.17	2.76	2.34	4.48	1.53, 1.66	$\delta\text{CH}_2$ : 1.38, 1.45; $\varepsilon\text{CH}_2$ : 1.52 $\zeta\text{CH}_2$ : 3.09, 3.38; $\eta\text{NH}$ : 7.99
$\beta^3$ -Orn3	$\text{H}_2\text{O}$	7.73	2.15	2.29	4.05	1.31, 1.43	$\delta\text{CH}_2$ : 1.48; $\varepsilon\text{CH}_2$ : 2.83
	MeOH	8.35	2.66	2.39	4.28	1.61, 1.63	$\delta\text{CH}_2$ : 1.49; $\varepsilon\text{CH}_2$ : 2.84, 2.90
$\beta^3$ -Val4	$\text{H}_2\text{O}$	7.69	2.20	2.37	3.81	1.58	$\delta\text{CH}_3$ : 0.77
	MeOH	8.18	2.57	2.44	4.12	1.72	$\delta\text{CH}_3$ : 0.93
$\beta^3$ -Asp5	$\text{H}_2\text{O}$	8.01	2.31	2.45	4.42	2.13, 2.22	
	MeOH	8.62	2.59	2.78	4.59	2.30, 2.30	
$\beta^3$ -Ser6	$\text{H}_2\text{O}$	7.97	2.22	2.27	4.02	3.29	
	MeOH	7.85	2.27	2.50	4.32	3.35, 3.45	
$\beta^3$ -Tyr7	$\text{H}_2\text{O}$	7.76	2.13	2.32	4.23	2.40, 2.67	$\varepsilon\text{H}$ : 6.95; $\zeta\text{H}$ : 6.64
	MeOH	7.64	2.12	2.41	4.48	2.60	$\varepsilon\text{H}$ : 6.95; $\zeta\text{H}$ : 6.63



gradients correspond to: Lys1 H<sup>n</sup> -5.8 ppb K<sup>-1</sup>; Val2 -2.5 ppb K<sup>-1</sup>; Orn3 -4.2 ppb K<sup>-1</sup>; Asp4 -2.5 ppb K<sup>-1</sup>; Val5 0.00 ppb K<sup>-1</sup>; Ser6 -6.7 ppb K<sup>-1</sup>; Tyr7 -7.5 ppb K<sup>-1</sup>. It is commonly assumed that coefficients more positive than -6 ppb K<sup>-1</sup> indicate intramolecular H-bonded H<sup>N</sup> protons in aqueous solution. The N-terminal five amino acids of the (1,4) lactam-bridged peptide **12b** showed all coefficients higher than -6 ppb K<sup>-1</sup>, thereby suggesting stabilization of the  $\beta$ -peptide backbone by the cyclization.

## Structure calculation of a cyclic $\beta^3$ -peptide

Based on a comparison of the CD data (Fig. 1) and the ROESY peak pattern (Supporting Information<sup>†</sup>), the 14-helix fold of the (2,5) lactam bridged  $\beta^3$ -peptide **8b** is highly similar in both solvents. The presence of certain 14-helix typical NOE-correlations for the same peptide in water, were already reported earlier.<sup>12b</sup> Based on the ROESY data recorded in methanol, it was possible to calculate a high-resolution NMR 3D structure of the (2,5) lactam bridged  $\beta^3$ -peptide **8b** (Fig. 8). The ROESY data in methanol was used, because the NMR signals were overall better resolved (Supporting Information<sup>†</sup>). Presumably due to higher conformational flexibility and/or increased exchange of the backbone amide with solvent protons, the ROESY data for the peptide in water showed overall weaker and thereby also about 20% fewer cross peaks. Moreover, NOE-restraints involving the backbone C <sup>$\beta$</sup> -proton around 4–5 ppm of the  $\beta^3$ -amino acid could be more reliably derived since the respective cross peaks were not disturbed by a strong water signal at about 4.7 ppm. The influence of water compared to methanol on the 14-helix fold was estimated from a refinement of the structures calculated based on the methanol restraints in water. This appeared valid due to the above mentioned similarity of the fold in both solvents.

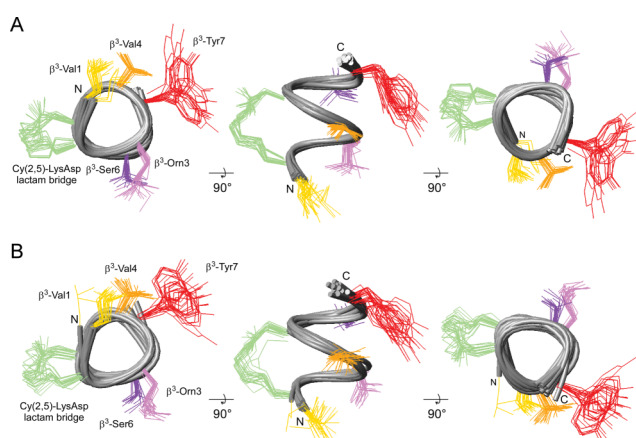


**Fig. 8** Superimposition of the 20 lowest energy structures of the (2,5) lactam bridged  $\beta^3$ -heptapeptide **8b** calculated based on the data recorded in methanol. The structures calculated *in vacuo* (A) represent the conformation in methanol. Subsequent refinement in a water-shell was done to obtain a structural model for the conformation in aqueous solvent (B). This approach appeared valid due to the high similarity of the folds in both solvents that is indicated by the presented CD and NMR data. Each bundle is shown in three different perspectives (bottom view, front view, top view). The grey tube in each bundle represents the backbone of the 14-helix. The side-chains on the three different regions on the 14-helix are given in different color-coding with the lactam bridge shown in green.

All structure calculations were performed with XPLOR-NIH<sup>18</sup> using torsion angle and Cartesian coordinate space molecular dynamics. The parameter and topology files “parallhdg.pro” and “topallhdg.pro” were modified to incorporate structural parameters (bonds, angles, dihedral angles, improper angles, charge *etc.*) for the  $\beta$ -amino acids appearing in the sequence of the cyclic  $\beta^3$ -heptapeptide **8b** and included in the Supporting Information.<sup>†</sup> Cyclization between the side-chains of  $\beta^3$ -hLys2 and  $\beta^3$ -hAsp5 was enabled by defining a new patch, which is similar to the one used for the definition of disulfide bonds. In addition, the distance between the side-chain amide nitrogen (N<sup>n</sup> of  $\beta^3$ -hLys2) and the side-chain C <sup>$\delta$</sup>  of  $\beta^3$ -hAsp5 was restrained to 1.5–5.3 Å. For one set of calculations, the ROEs were calibrated exactly according to the ROE cross peak intensity, which is referred to a ‘calibrated’. For a second set of calculations the cross peak intensities were used to simply group the ROEs into 4 bins with upper bounds set to 2.3 Å, 2.8 Å, 3.6 Å, and 5.8 Å, respectively. This is referred to as ‘bin’. The lower bound corresponded approximately to the sum of the van der Waals radii. For all distance restraints  $r^{-6}$  sum averaging was used. In addition, stereo-specific assignments were obtained for all  $\alpha$ -methylene proton pairs.

A total of 121 distance restraints were derived from unambiguous ROE assignments (Table 2), which corresponds to about 17 restraints per residue. Hydrogen bonds restraints were defined based on hydrogen-deuterium exchange experiments and the observed ROE correlations. The H<sup>N</sup>-O distance bounds for residue pairs 2–4, 3–5, 4–6 and 5–7 were 1.8–2.3 Å. We also performed a run without hydrogen bonds restraints as a reference, leading to the same overall fold (see Supporting Information<sup>†</sup>). The 20 lowest

**Table 2** Statistics of the 20 lowest energy structures of **8b**, calculated based on data recorded in methanol

Type of distance restraint	Calibrated	Bin definition
Distance restraints		
Total	125	125
Intraresidue	86	86
Sequential	13	13
Medium range	22	22
Hydrogen bond restraints	4	4
<b>For the structure calculation in vacuo<sup>a</sup></b>		
Rmsd's from experimental restraints		
Distance (Å)	0.0477 ± 0.0021	0.0323 ± 0.0031
Rmsd's from idealized geometry		
Bonds	0.0044 ± 0.0002	0.0034 ± 0.0004
Angles	0.5383 ± 0.0147	0.480 ± 0.019
Improper	0.257 ± 0.022	0.210 ± 0.018
Lennard-Jones energy (kcal mol <sup>-1</sup> )	-13.5 ± 4.1	-12.5 ± 2.9
Average rmsd to mean structure (Å)		
Residues 1–7 (bb/heavy)	0.42/0.84	0.61/1.20
<b>Following the refinement in a water shell<sup>a</sup></b>		
Rmsd's from experimental restraints		
Distance (Å)	0.0349 ± 0.0020	0.0270 ± 0.0020
Rmsd's from idealized geometry		
Bonds	0.0094 ± 0.0007	0.0097 ± 0.0006
Angles	1.309 ± 0.0605	1.097 ± 0.063
Improper	0.450 ± 0.067	0.421 ± 0.065
Total energy (kcal mol <sup>-1</sup> )	-98.8 ± 10.2	-91.5 ± 14.8
Average rmsd to mean structure (Å)		
Residues 1–7 (bb/heavy)	0.34/0.74	0.49/1.04

<sup>a</sup> None of the structures had distance restraints violations > 0.5 Å, rms(d) = root mean square (deviation), bb = backbone (CA, CB, C, O, N).

energy structures out of 200 calculated ones were additionally refined in a water-shell (Fig. 8b).<sup>19</sup> Structural statistics are given in Table 2. As described above, refinement of the structure in a water shell was performed to achieve a model of the structure that allows to estimate the behaviour in aqueous solution (Fig. 8b).

The water-refined NMR structures of  $\beta^3$ -peptide **8b** showed all a well-defined compact 14-helix structure with only little fraying of the backbone at the N- and C-termini. A full helix turn is achieved every three residues and side-chains are superimposed in three different segments around the helical axis. Only the side-chains of the N-terminal  $\beta^3$ -hVal and the C-terminal  $\beta^3$ -hTyr show somewhat more structural heterogeneity, in line with the specific position of the lactam bridge. The lactam bridge occupies one of the three flanking sites and is thus fully consistent with the hydrogen bonding pattern in the 14-helix. As seen from the surface display, the peptide appears very compact due to the cyclization and the small number of seven residues (Fig. 9). As such, despite the 14-helix formation, a highly compact folded structure is formed. The lactam bridge significantly limits the number of possible  $\beta^3$ -peptide conformations, which is reflected in low backbone rmsd values (Table 2), thereby stabilizing the 14-helix backbone structure. This suggests that the respective structure could serve as a scaffold for the positioning of side-chains in a highly ordered 3D format. Such high order for the side-chains has already previously been noted in a comparative study with  $\beta$ -peptides incorporating six-membered ring constrained residues.<sup>12b</sup>

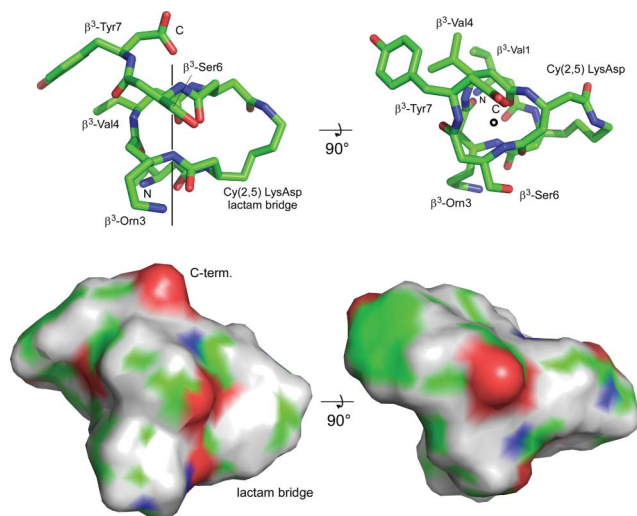


**Fig. 9** Structure of one lowest energy conformation of the cyclic 14-helix **8b** peptide as calculated from NMR data recorded in MeOH. Shown are two different perspectives as stick (top) and as surface representation (bottom). Despite 14-helix formation, the molecule appears compact but not elongated due to the (2,5) lactam bridge and the short size of seven residues. Note that the NH...OC hydrogen bond pairing in the backbone of the  $3_{14}$   $\beta^3$ -peptide is in opposite direction to those of the conventional  $3_{6,13}$   $\alpha$  peptide helix, giving the helix an opposite dipolar character. The positions of specific amino acids and functions are added for clarity. The helical axis is indicated in the stick model for clarity.

## Conclusions

The folding of  $\beta$ -peptides into specific secondary structures can nowadays be controlled to a great extent. Nevertheless, stable

folding of  $\beta$ -peptides in water remains a challenge. This is especially true for short  $\beta$ -peptides, featuring only a limited number of  $\beta$ -amino acids for fold stabilization. In this manuscript we addressed this issue for the folding of  $\beta$ -peptide heptamers in a 14-helical secondary structure in water. The incorporation of a single lactam bridge, which connects two  $\beta$ -amino acid side-chains, in the  $\beta$ -heptapeptide leads to high 14-helix character in water. By executing a comparative study on a library of  $\beta$ -heptapeptides, with varying lactam bridge positions, orientations and lengths, the optimal placement of the stabilizing motif on the  $\beta^3$ -peptide scaffold could be deduced. CD and NMR spectroscopy, together with structure calculations, revealed that the optimal position for inducing 14-helicity is located at the N-terminus of the  $\beta$ -peptide, and therewith markedly contrasts with the effects of a more classical side-chain-to-side-chain salt-bridge. The lactam bridge is ideally incorporated in the N-terminal region of the  $\beta^3$ -peptide, because the conformational flexibility of the peptide backbone is intrinsically the highest at this position. Stabilization of this specific segment with a lactam bridge leads to the highest overall 14-helicity. The lactam bridge induces a 14-helical conformation in methanol and water to a similar extent and with high order, both in the backbone and in the side-chains, leading to a highly compact and stable folded structure.

The presented first high-resolution NMR structure of the (2,5) lactam bridged  $\beta^3$ -heptapeptide **8b** is very compact. A lactam bridge of appropriate length and position significantly limits the number of  $\beta^3$ -peptide conformations, thereby stabilizing the 14-helix backbone structure even in a very short peptide of only seven residues. Even though the reported  $\beta^3$ -heptapeptides are model peptides, the results imply that this small and stable 14-helical  $\beta^3$ -peptide fold could serve as a stable scaffold for the positioning of functionally important side-chains on a rigid backbone structure for biologically active  $\beta^3$ -peptide sequences, e.g. for applications in the area of protein recognition or membrane targeting. Moreover, stabilization by covalent cyclization might be particularly suited to minimize proteolytic digest in cells or blood and to enhance membrane transport.

## Acknowledgements

We thank Bernhard Griewel for expert technical assistance with NMR measurements and Ingrid Vetter for helpful discussions on template building. This work was supported by a Sofja Kovalevskaja Award from the Alexander von Humboldt Foundation and the BMBF to L.B. and the Spanish Ministerio de Educación y Ciencia (postdoctoral fellowship E.V.).

## Notes and references

- (a) S. H. Gellman, *Acc. Chem. Res.*, 1998, **31**, 173–180; (b) K. Kirshenbaum, R. N. Zuckermann and K. A. Dill, *Curr. Opin. Struct. Biol.*, 1999, **9**, 530–535; (c) D. J. Hill, M. J. Mio, R. B. Prince, T. S. Hughes and J. S. Moore, *Chem. Rev.*, 2001, **102**, 3892–4011; (d) *Foldamers: Structure, Properties, and Applications*, S. Hecht and I. Huc, ed., Wiley-VCH, New York, 2007.
- (a) R. P. Cheng, S. H. Gellman and W. F. DeGrado, *Chem. Rev.*, 2001, **101**, 3219–3232; (b) D. Seebach, D. F. Hook and A. Glattli, *Biopolymers*, 2006, **84**, 23–37; (c) C. M. Goodman, S. Choi, S. Shandler and W. F. DeGrado, *Nat. Chem. Biol.*, 2007, **3**, 252–262; (d) A. D. Bautista, C. J. Craig, E. A. Harker and A. Schepartz, *Curr. Opin. Chem. Biol.*, 2007, 685–692.



- 3 (a) M. Werder, H. Hauser, S. Abele and D. Seebach, *Helv. Chim. Acta*, 1999, **82**, 1774–1783; (b) K. Gademann, M. Ernst, D. Hoyer and D. Seebach, *Angew. Chem., Int. Ed.*, 1999, **38**, 1223–1226; (c) E. A. Porter, X. Wang, H. S. Lee, B. Weisblum and S. H. Gellman, *Nature*, 2000, **404**, 565; (d) M. Rueping, Y. Mahajan, M. Sauer and D. Seebach, *ChemBioChem*, 2002, **3**, 257–259; (e) T. B. Potocky, A. K. Menon and S. H. Gellman, *J. Biol. Chem.*, 2003, **278**, 50188–50194; (f) M. A. Gellman, S. Richter, H. Cao, N. Umezawa, S. H. Gellman and T. M. Rana, *Org. Lett.*, 2003, **5**, 3563–3565; (g) E. P. English, R. S. Chumanov, S. H. Gellman and T. Compton, *J. Biol. Chem.*, 2006, **281**, 2661–2667; (h) Y. D. Wu, W. Han, D. P. Wang, Y. Gao and Y. L. Zhao, *Acc. Chem. Res.*, 2008, **41**, 1418–1427; (i) S. J. Shandler, M. V. Shapovalov, R. L. Dunbrack and W. F. DeGrado, *J. Am. Chem. Soc.*, 2010, **132**, 7312–7320.
- 4 (a) D. Seebach, M. Overhand, F. N. M. Kuhnle, B. Martinoni, L. Oberer, U. Hommel and H. Widmer, *Helv. Chim. Acta*, 1996, **79**, 913–941; (b) D. Seebach, A. K. Beck and D. J. Bierbaum, *Chem. Biodiversity*, 2004, **1**, 1111–1239; (c) B. Keller, Z. Gattin and W. F. van Gunsteren, *Proteins: Struct., Funct., Bioinform.*, 2010, **78**, 1677–1690; (d) G. Montalvo, M. M. Waegle, S. Shandler, F. Gai and W. F. DeGrado, *J. Am. Chem. Soc.*, 2010, **132**, 5616–5618.
- 5 (a) M. Werder, H. Hauser, S. Abele and D. Seebach, *Helv. Chim. Acta*, 1999, **82**, 1774–1783; (b) J. A. Kritzer, J. D. Lear, M. E. Hodsdon and A. Schepartz, *J. Am. Chem. Soc.*, 2004, **126**, 9468–9469; (c) J. A. Kritzer, N. W. Luedtke, E. A. Harker and A. Schepartz, *J. Am. Chem. Soc.*, 2005, **127**, 14584–14585; (d) O. M. Stephens, S. Kim, B. D. Welch, M. E. Hodsdon, M. S. Kay and A. Schepartz, *J. Am. Chem. Soc.*, 2005, **127**, 13126–13127; (e) J. A. Kritzer, O. M. Stephens, D. A. Guarracino, S. K. Reznik and A. Schepartz, *Bioorg. Med. Chem.*, 2005, **13**, 11–16; (f) J. A. Kritzer, M. E. Hodsdon and A. Schepartz, *J. Am. Chem. Soc.*, 2005, **127**, 4118–4119; (g) J. K. Murray, B. Farooqi, J. D. Sadowsky, M. Scalf, W. A. Freund, L. M. Smith, J. Chen and S. H. Gellman, *J. Am. Chem. Soc.*, 2005, **127**, 13271–13280; (h) E. P. English, R. S. Chumanov, S. H. Gellman and T. Compton, *J. Biol. Chem.*, 2006, **281**, 2661–2667; (i) J. K. Murray and S. H. Gellman, *Biopolymers*, 2007, **88**, 657–686; (j) E. A. Harker, D. S. Daniels, D. A. Guarracino and A. Schepartz, *Bioorg. Med. Chem. Lett.*, 2009, **19**, 3736–3738; (l) E. F. Lee, J. D. Sadowsky, B. J. Smith, P. E. Czabotar, K. J. Peterson-Kaufman, P. M. Colman, S. H. Gellman and W. D. Fairlie, *Angew. Chem., Int. Ed.*, 2009, **48**, 4318–4322.
- 6 (a) Y. Hamuro, J. P. Schneider and W. F. DeGrado, *J. Am. Chem. Soc.*, 1999, **121**, 12200–12201; (b) T. L. Raguse, E. A. Porter, B. Weisblum and S. H. Gellman, *J. Am. Chem. Soc.*, 2002, **124**, 12774–12785; (c) D. Liu and W. F. DeGrado, *J. Am. Chem. Soc.*, 2001, **123**, 7553–7559; (d) R. F. Epand, T. L. Raguse, S. H. Gellman and R. M. Epand, *Biochemistry*, 2004, **43**, 9527–9535; (e) A. J. Karlsson, W. C. Pomerantz, B. Weisblum, S. H. Gellman and S. P. Palecek, *J. Am. Chem. Soc.*, 2006, **128**, 12630–12631; (f) A. J. Karlsson, W. C. Pomerantz, K. J. Neilsen, S. H. Gellman and S. P. Palecek, *ACS Chem. Biol.*, 2009, **4**, 567–579; (g) A. J. Karlsson, R. M. Flessner, S. H. Gellman, D. M. Lynn and S. P. Palecek, *Biomacromol.*, 2010, **11**, 2321–2328; (h) J. Mondal, X. Zhu, Q. Cui and A. Yethiraj, *J. Phys. Chem. B*, 2010, **114**, 13585–13592.
- 7 (a) D. H. Appella, J. J. Barchi, S. R. Durell and S. H. Gellman, *J. Am. Chem. Soc.*, 1999, **121**, 2309–2310; (b) T. L. Raguse, J. R. Lai and S. H. Gellman, *J. Am. Chem. Soc.*, 2003, **125**, 5592–5593; (c) M. Lee, T. L. Raguse, M. Schinnerl, W. C. Pomerantz, X. Wang, P. Wipf and S. H. Gellman, *Org. Lett.*, 2007, **9**, 1801–1804.
- 8 (a) P. I. Arvidsson, M. Rueping and D. Seebach, *Chem. Commun.*, 2001, 649–650; (b) R. P. Cheng and W. F. DeGrado, *J. Am. Chem. Soc.*, 2001, **123**, 5162–5163.
- 9 (a) T. L. Raguse, J. R. Lai and S. H. Gellman, *Helv. Chim. Acta*, 2002, **85**, 4154–4164; (b) S. A. Hart, A. B. F. Bahadoor, E. E. Matthews, X. Y. J. Qiu and A. Schepartz, *J. Am. Chem. Soc.*, 2003, **125**, 4022–4023; (c) J. A. Kritzer, J. Tirado-Rives, S. A. Hart, J. D. Lear, W. L. Jorgensen and A. Schepartz, *J. Am. Chem. Soc.*, 2005, **127**, 167–178.
- 10 (a) A. K. Galande, K. S. Bramlett, J. O. Trent, T. P. Burris, J. L. Wittliff and A. F. Spatola, *ChemBioChem*, 2005, **6**, 1991–1998; (b) L. K. Henchley, A. L. Jochim and P. S. Arora, *Curr. Opin. Chem. Biol.*, 2008, **12**, 692–697.
- 11 (a) A. Jacobi and D. Seebach, *Helv. Chim. Acta*, 1999, **82**, 1150–1172; (b) M. Rueping, B. Jaun and D. Seebach, *Chem. Commun.*, 2000, 2267–2268.
- 12 (a) E. Vaz and L. Brunsveld, *Org. Lett.*, 2006, **8**, 4199–4202; (b) E. Vaz, W. C. Pomerantz, M. Geyer, S. H. Gellman and L. Brunsveld, *ChemBioChem*, 2008, **9**, 2254–2259.
- 13 M.-O. Ebert, J. Gardiner, S. Ballet, A. D. Abell and D. Seebach, *Helv. Chim. Acta*, 2009, **92**, 2643–2658.
- 14 (a) Y. E. Bergman, M. P. Del Borgo, R. D. Gopalan, S. Jalal, S. E. Unabia, M. Ciampini, D. J. Clayton, J. M. Fletcher, R. J. Mulder, J. A. Wilce, M.-I. Aguilar and P. Perlmutter, *Org. Lett.*, 2009, **11**, 4438–4440; (b) A. D. Bautista, J. S. Appelbaum, C. J. Craig, J. Michel and A. Schepartz, *J. Am. Chem. Soc.*, 2010, **132**, 2904–2906.
- 15 J. W. Taylor, *Biopolymers*, 2002, **66**, 49–75.
- 16 D. H. Appella, L. A. Christianson, I. L. Karle, D. R. Powell and S. H. Gellman, *J. Am. Chem. Soc.*, 1996, **118**, 13071–13072.
- 17 K. Gademann, B. Jaun, D. Seebach, R. Perozzo, L. Scapozza and G. Folkers, *Helv. Chim. Acta*, 1999, **82**, 1–11.
- 18 C. D. Schwieters, J. J. Kuszewski, N. Tjandra and G. M. Clore, *J. Magn. Reson.*, 2003, **160**, 65–73.
- 19 (a) J. P. Linge, M. A. Williams, C. A. Spronk, A. M. Bonvin and M. Nilges, *Proteins: Struct., Funct., Genet.*, 2003, **50**, 496–506; (b) S. B. Nabuurs, A. J. Nederveen, W. Vranken, J. F. Doreleijers, A. M. Bonvin, G. W. Vuister, G. Vriend and C. A. Spronk, *Proteins: Struct., Funct., Bioinf.*, 2004, **55**, 483–486.